On the length scale and Strouhal numbers for sound transmission across coupled duct cavities at low Mach number

S.K. Tang[a)] and Yijia Tang[b)]

Department of Building Environment and Energy Engineering
The Hong Kong Polytechnic University
Hong Kong, China

[a)] Author to whom correspondence should be addressed.
Electronic mail: shiu-keung.tang@polyu.edu.hk

[b)] Now at College of Internet of Things Engineering, Guangdong Polytechnic of Science and Technology, Guangzhou 510640, China

Abstract

The sound transmission across two coupled cavities along a rectangular duct in the presence of a low Mach number flow is examined experimentally in the present study. Effort is also made for deeper understanding on how the flow, the excitation sound frequency and the excitation level influence the sound transmission loss. Results confirm that the high sound transmission loss across the cavities is associated with the strong out-of-phase pressure fluctuations within the cavities. The sound transmission loss deteriorates significantly once the flow speed exceeds a threshold value. A new length scale is proposed. This length scale, together with the threshold flow speed and the peak sound transmission loss frequency, gives a Strouhal number which is basically independent of the cavity offset for a fixed cavity length. The present finding extends the previous effort of the authors, enabling the prediction of the flow speed limit and the operating frequency of coupled cavities for duct silencing at low Mach number.

PACS numbers : 43.50.Gf, 43.28.Py, 43.20.Mv

Keywords :

Duct noise control; sound propagation; reactive silencer; flow-acoustics-structure interaction

I. INTRODUCTION

Ventilation system noise in modernized buildings has long been a problem in building noise control. This type of noise will propagate along the ductwork and enter the occupied zones of the buildings, resulting in poor indoor acoustical quality, which will eventually lead to health problems and lower productivity, if they are not attenuated properly.[1] Though there are noise criteria which help limit the noise exposure of building occupants (for instance, Beranek[2] and Hay and Kemp[3]), the development of effective flow duct silencers has been attracting great attentions of engineers and academics for many façades.

The traditional flow duct silencer is of the dissipative type, which is basically a flow constriction with porous materials installed on the two sides of the constriction.[4] However, the low frequency performance of this silencer type is not satisfactory because of the properties of the porous materials. The flow constriction also gives rise to a significant static air pressure drop across the silencer so that a more powerful but noisier fan is often required to deliver the required air flow rate. Besides, this silencer type is not suitable for application in locations where a high hygiene standard is to be maintained because the deterioration of the porous materials will result in increased air particulate in the indoor air. Neither is this type of silencer suitable for applications where the air is dirty/greasy. The drum-like silencer proposed by Huang and Choy[5] is also not applicable in such condition and the maintenance of the tension in the membrane is not straight-forward. Flow duct silencers containing micro-perforated absorbers, such as that of Allam and Åbom,[6] suffer similar drawback. Active control technique has been implemented in the ventilation systems,[7] but the reliability of the microphone signals in the relatively hostile duct interior remains a big challenge to the professionals.

The development of passive reactive silencers, which do not contain any flexible structure, has also been a hot research topic. Typical examples include the Helmholtz resonators,[8] the expansion chambers/plenum chambers,[9] the Herschel-Quincke tubes[10] and conical tube resonators.[11] One major drawback of this silencer type is that it can only give satisfactory performance at or close to its resonance frequency. Coupled resonators, such as those of Seo and Kim[12] and Howard et al.,[13] can give wider working bandwidths. Recently, Howard and Craig,[14] Tang,[15] Yu and Tang[16] and Červenka and Bednařík[17] proposed the use of sidebranches as silencing devices. However, coupling reactive devices will lead to bulky setup, which is not desirable in the view of the limited ceiling voids available for their installation in practice. Their manufacturing is also not going to be straight-forward.

The recent work of Tang and Tang[18] reveals the possibility of creating broadband silencing by coupling two cavities along a rectangular duct. This setup is very simple and is basically that of an expansion chamber with its two cavities offset in the flow direction. It is found that the longer the offset distance, the stronger the sound transmission loss. Also, the cavities need not to be large. Leung et al.[19] investigated numerically the aeroacoustics of such setup at transonic Mach numbers, and the cavities they adopted were long enough for the shear layers to roll up into individual vortices. A more recent work of Tang and Tang[20] illustrates the mechanisms of the abovementioned high sound transmission loss and relates explicitly the stopband cut-on frequency to the dimensions of the coupled cavities and the duct in the absence of a duct flow.

Similar to other ducted elements, such as those studied by Yu and Tang,[16] Tang,[21] Davies and Holland[22] and Tonon et al.,[23] the performance of the coupled duct cavities is expected to be worsen in the presence of a duct flow. Flow-induced noise is a big problem of duct silencers, regardless of their being dissipative or reactive.[24,25] However, the results of Tang[21] illustrate that there is a critical flow speed over which the performance of his resonators will start to deteriorate, but the issue of how such velocity is related to the resonator configurations has not been addressed. Similar phenomenon is also observed in Yu and Tang.[16]

In this study, a series of experiments is derived to study how the sound transmission loss across the coupled cavities is affected by the presence of a low Mach number duct flow. Effort is also made on understanding the critical duct flow velocity over which deterioration of sound transmission loss will be resulted, and how this velocity is related to the peak transmission loss

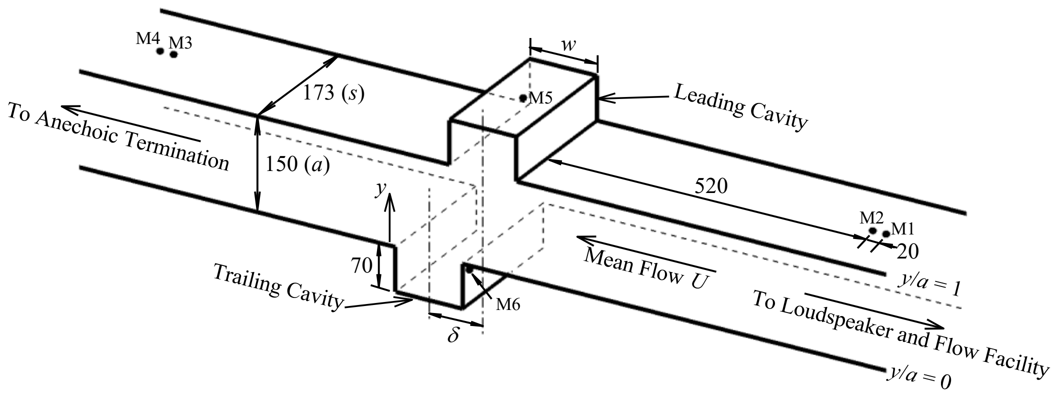

FIG. 1. Schematics and dimensions of the coupled cavity section. All dimensions in mm.
● : Microphone

frequency and the cavity dimensions. These results, together with the previous effort of the authors,[20] will help establish a framework for the design of coupled cavities as a flow duct silencing device. For practical building application reasons, the cavities adopted in this study are kept narrow so that the proposed device is compact and simple.

II. EXPERIMENTAL SETUP

The test rig of the present study was that of Yu and Tang[16] except that their sidebranch array muffler was replaced by two rectangular coupled cavities. It was made of 20 mm thick Perspex panels in order to avoid adverse effect of duct/cavity wall vibration. Figure 1 shows the schematics and internal dimensions of the test section, the nomenclature and the locations of the sensors. The first higher mode was that associated with the duct span s (= 173 mm) and its cut-on frequency was around 990 Hz. The highest frequency of interest in this study was actually below 800 Hz so that one could basically assume that all the evanescent waves at the microphone locations were insignificant and the waves should be essentially planar at the locations of the microphones M1 to M4. These microphones were installed symmetrically about the centerline of the leading cavity. A fan and a loudspeaker with a circular aperture comparable to the duct span were installed at the upstream end of the test section as in Tang.[21] The latter was capable of producing sounds with magnitude not less than 100 dB over the whole frequency range of interest. The background noise in the laboratory during the experiment was negligible compared to the artificial sound level created by the loudspeaker.

An absorptive ending, designed according to the recommendations of Neise et al.,[26] was attached to the downstream end of the test rig to minimize sound reflection there. The coefficient of sound power reflection by this absorptive ending was less than 0.03 for frequencies higher than 200 Hz.[21] The cavities adopted in the present study can be regarded as 'narrow' with w = 100 mm and 70 mm. Given a smaller cavity length w than the duct width a, the type of planar longitudinal wave interactions inside traditional expansion chambers, whose lengths are long compared to the duct widths (for instance, Munjal[9]), did not take place in this study. This has already been illustrated in Tang and Tang,[20] and thus is not discussed further.

The sound power transmission losses, TLs, in this study were estimated from the signals obtained by the four wall-mounted ¼" microphones (M1 to M4, Brüel & Kjær Type 4935) using the four-microphone method. This method has been presented in detail in Tang and Li[27] and thus is not repeated here. These microphones were far enough from the coupled cavities to avoid the contamination of the evanescent waves. The separation between the microphones in each pair was set at 20 mm (27 mm in Chung and Blaser[28]). A trial test was done using a separation of 80 mm with w = 100 mm. The corresponding spectral sound transmission losses do not show significant difference from those measured using a 20 mm microphone separation within 500 Hz to 800 Hz (not shown here), which is the main frequency range of interest in this study, even when U was as high as 16 m/s. M5 and M6 were located at the centres of the cavity ceilings. The data recorder was a Brüel & Kjær Type 3506D PULSE system. The sampling rate was 4096 samples per second per channel throughout the measurements.

The average longitudinal air velocity across the duct cross-section, U, was varied from 0 and 20 m/s in intervals of 2 m/s. The distance of the leading edge of the leading cavity from the flow entry was about 2 m. The boundary layer at this leading edge should not be laminar even for the case of U = 2 m/s. The air velocity was measured by a TFI Series 100 cobra probe (head width 2.6 mm) upstream of the test section on a vertical plane near to the upstream microphones. This probe was removed during the sound transmission measurements. The air turbulence intensities on the duct centerline on that vertical plane was ~3% of the main longitudinal flow speed U. The mean transverse flow velocities in the main duct were negligible. A single hotwire facing normally to the longitudinal main flow direction was used to measure the longitudinal flow velocity and turbulence intensity profiles across the cavity shear layers.[29]

The loudspeaker was turned on and fed with a white noise signal during the TL measurements with and without flow. The sound pressures at M1 and M2 due to the loudspeaker were kept at least 82 dB (maximum ~ 100 dB) on average between 600 Hz to 800 Hz, which was the major working frequency ranges of the coupled cavities in the present study. This level of artificial sound pressure overrode that due to the flow generating facility in most of the cases. Signal contamination due to flow turbulence was possible when $U > 16$ m/s at low artificial excitation levels. Those results are not included in the data analysis.

III. RESULTS AND DISCUSSIONS

In this section, the effects of air flow velocity, U, and the offset distance, δ, on the TLs across the coupled cavity sections will be examined in details in the first place. The air flow velocity U was varied between 0 to 20 m/s in intervals of 2 m/s, while δ was increased from 0 mm to the full cavity length w in intervals of 10 mm. The present interests, apart from obtaining deeper understanding on the sound transmission loss across the coupled cavities, are to find out the threshold flow velocity for reduced cavity acoustical performance and then establish its relationship with cavity dimension and the frequency of peak sound transmission loss. In the foregoing discussions, all lengths and frequency, unless otherwise stated, are normalized by the duct width a and the first transverse odd mode cut-on frequency, f_1 (=1143.3 Hz), respectively.

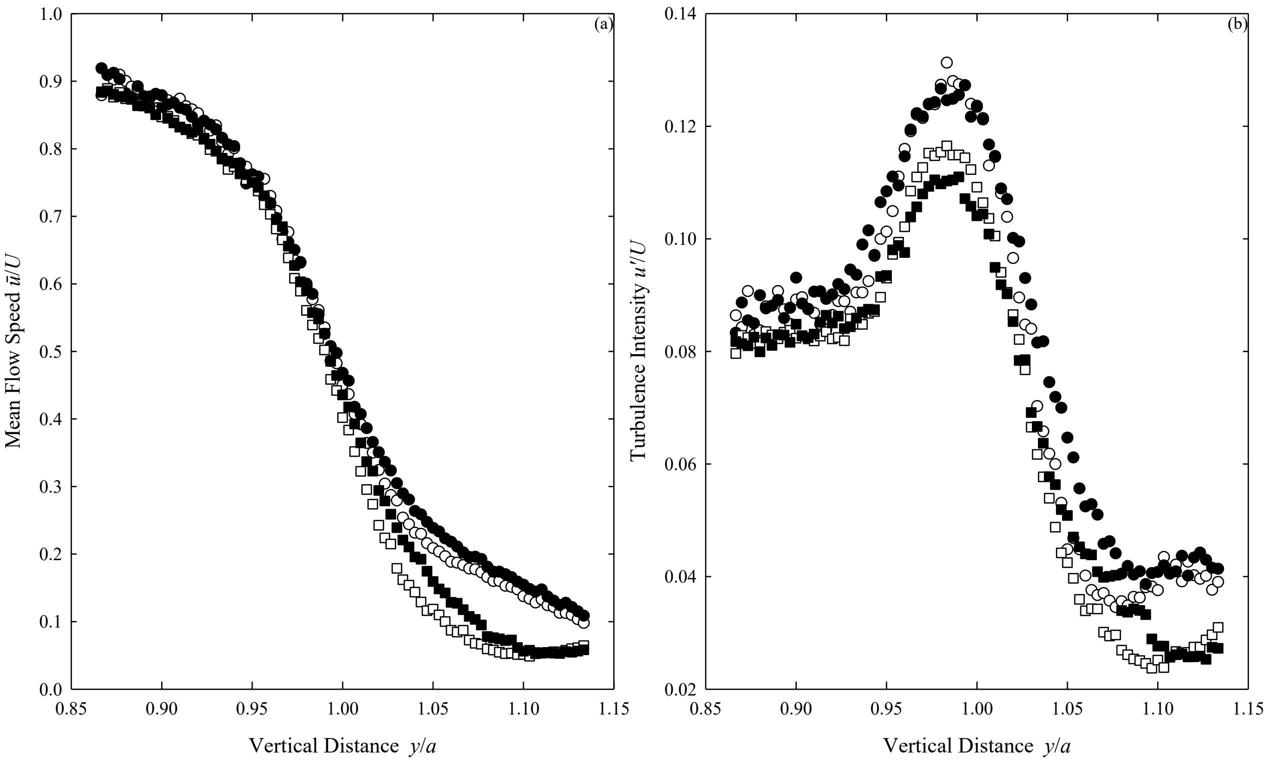

FIG. 2. Mean properties of the leading cavity shear layers, $\delta/w = 1$.
(a) Mean flow speed profile; (b) turbulence intensity profile.
● : $U = 4$ m/s; ■ : $U = 12$ m/s; open symbol : without artificial excitation;
closed symbol : overall artificial excitation level of 100 dB from 500 Hz to 1kHz.

A. Shear layer profiles

Figure 2(a) illustrates the vertical profile of the mean flow speed across the leading cavity shear layer on the vertical plane containing M5 (midway of the cavity-main flow interface) with and without excitation for the case of $\delta/w = 1$. The corresponding turbulence intensity profiles are presented in Fig. 2(b). The position $y/a = 1$ represents the cavity-main flow interface and $y/a > 1$ a position inside the cavity. It should be noted that the single hot-wire sensed both the longitudinal and transverse flow velocity components in the present study, but the mean component of the latter should be small compared to the main flow U. The turbulence intensity data include both the two abovementioned flow fluctuation components. u' denotes the root-mean-square value of the flow speed time fluctuations.

The results in Fig. 2 show the essential features of a mixing layer.[30] The strongest turbulence intensity is observed near the location of the highest mean shear rate. It is observed that the artificial excitation tends to thicken a bit the shear layer into the cavity, reducing the mean shear rate. The

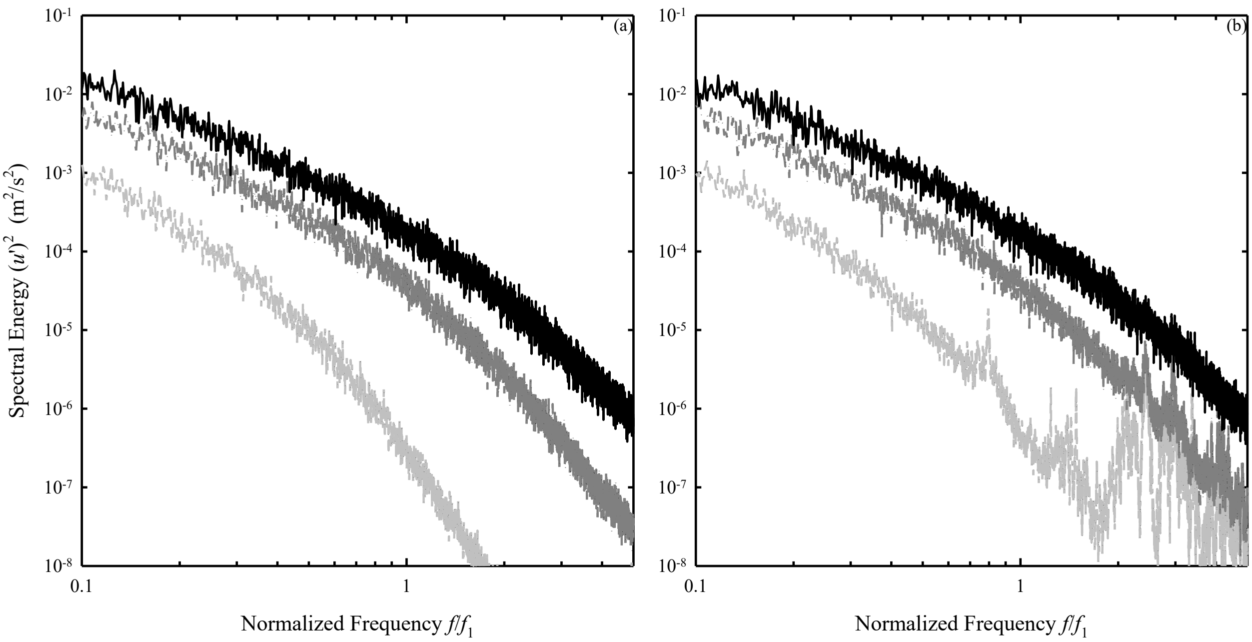

FIG. 3. Turbulence velocity spectra within the leading cavity shear layers, $\delta/w = 1$.
(a) Without artificial excitation;
(b) overall artificial excitation level of 100 dB from 500 Hz to 1kHz.
– – – – : U = 4 m/s; — · — : U = 8 m/s; ———— : U = 12 m/s.

shear layer thickening increases with excitation level (not shown here). This implies that a stronger mean flow speed U is required to maintain a given mean shear rate at increased excitation level.

It should be noticed that the turbulence intensity in the shear layer on the cavity-side is increased when an upstream artificial excitation is introduced, and it also increases with increasing excitation level (not shown here). Though this is rather expected, it can be observed that larger and more extensive increase of the turbulence intensity is associated with a lower U. One can even observe a reduction of the maximum turbulence intensity for the case of U = 12 m/s. This tends to suggest that the shear layer aerodynamics is more susceptible to change by the artificial upstream excitation at lower U. One can also conclude that a stronger U will result in a shear layer less vulnerable to acoustic excitation.

Figure 3 shows some turbulence spectra midway within the leading cavity shear layer for $\delta/w = 1$ and $y/a = 1$. Without the artificial excitation, the spectral intensity decays monotonically with frequency [Fig. 3(a)] within the frequency range of interest and they resemble those of static pressure fluctuations of a turbulent mixing layer.[31] The cavity shear layers are turbulent. Under excitation, there appears some organized motions at frequencies around $0.78f_1$, around $1.5f_1$ and between $2f_1$ to

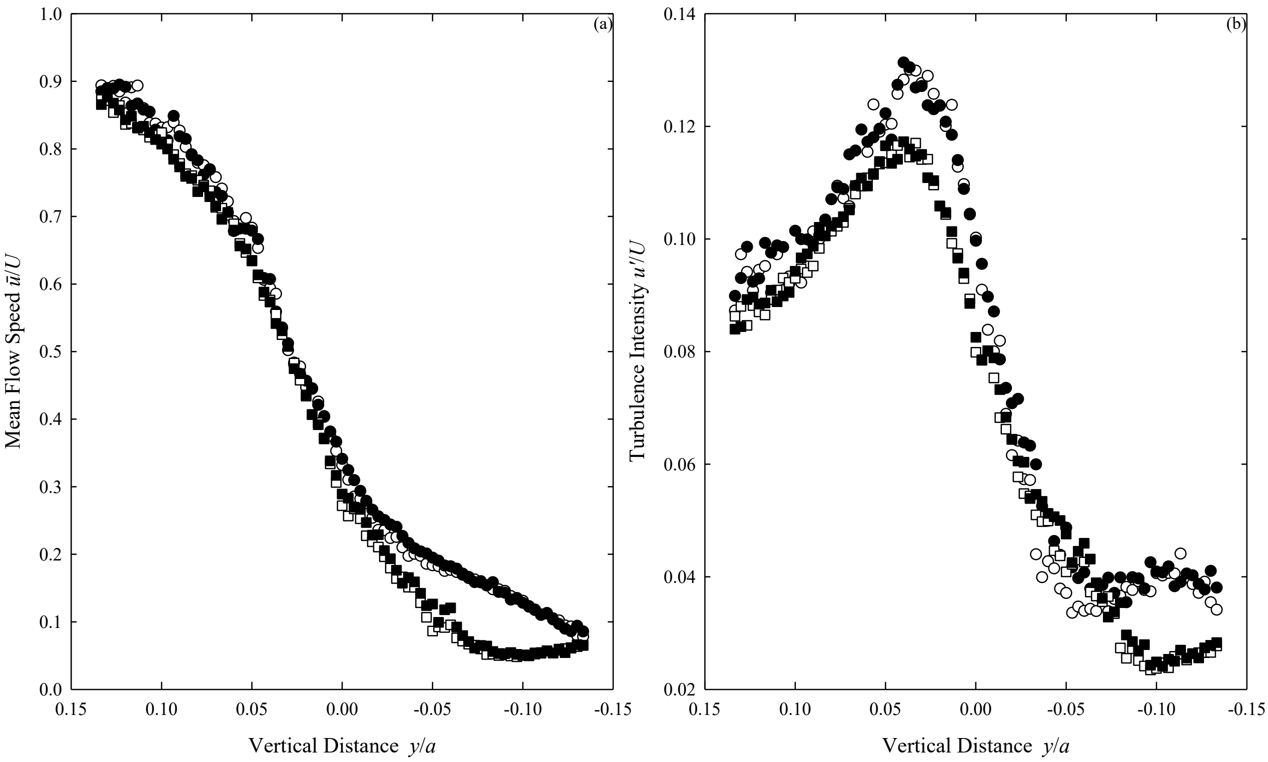

FIG. 4. Mean properties of the trailing cavity shear layers, $\delta/w = 1$.
(a) Mean flow speed profile; (b) turbulence intensity profile.
Legends : same as those of Fig. 2.

$3f_1$ for the case of $U = 4$ m/s [Fig. 3(b)]. Similar phenomenon can be observed for the case of $U = 8$ m/s, but only between the frequency range from $2f_1$ to $3f_1$. At $U = 12$ m/s, only a very small and insignificant spectral peak can barely be observed at ~$3f_1$. Apart from these peaks, the rest of these spectra is basically the same as those of their unexcited counterparts. The increase of turbulence level with increasing U tends to mask or dissipate the organized motions within the shear layers. Though the shear layers are likely to be excited and some organized fluid motions are resulted (more distinguishable at lower U), the effect is small and the frequencies of these motions do not match with the sound transmission loss peak frequencies to be discussed in Section III.B.

Figures 4(a) and 4(b) illustrate the mean flow speed and turbulence intensity profiles across the trailing cavity shear layer at its mid-length respectively for the case of $\delta/w = 1$. The vertical position of $y/a = 0$ represents the interface between the cavity and the main duct. Negative and positive y/a denotes position inside and outside the cavity respectively. Compared with the corresponding results of the leading cavity, it is observed that the trailing cavity shear layers have a slightly higher mean shear rate and are a bit more inwards into the main duct. It is also noticed that

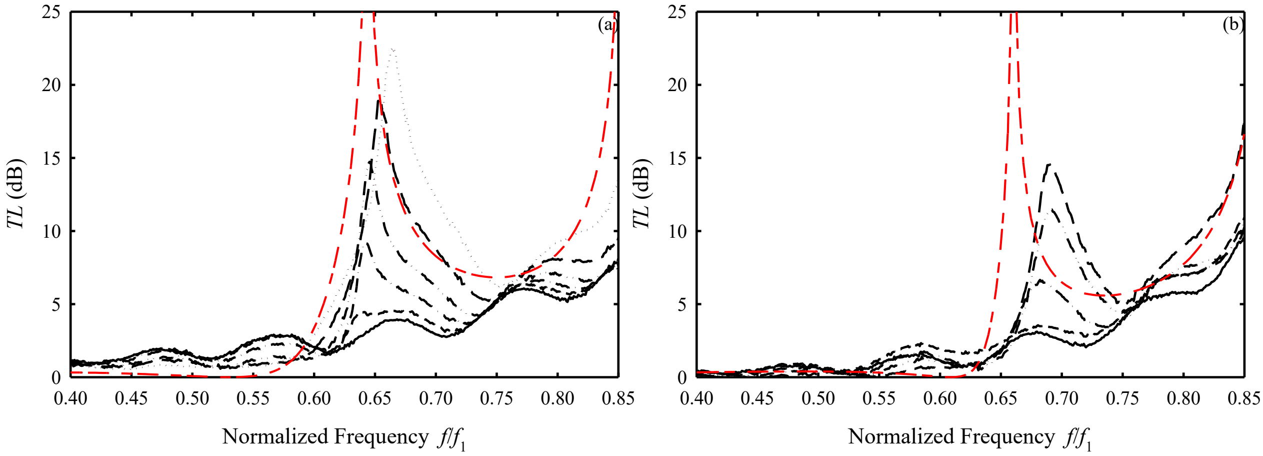

FIG. 5. (Color online) Spectral variations of the *TL*s across the coupled cavity regions for U = 0 m/s.
(a) w/a = 2/3;
———— : δ_r = 0; – – – – : δ_r = 0.2; — · — : δ_r = 0.4; — ·· — : δ_r = 0.6;
—— —— : δ_r = 0.8; ············ : δ_r = 1; — — — : δ_r = 1 (Finite element simulation).
(b) w/a = 7/15;
———— : δ_r = 0; – – – – : δ_r = 2/7; — · — : δ_r = 4/7; — ·· — : δ_r = 6/7;
—— —— : δ_r = 1; — — — : δ_r = 1 (Finite element simulation).

the trailing cavity shear layers are less affected by the artificial excitation than their leading cavity counterparts. This tends to imply that the leading cavity plays a more important role in the aeroacoustical behaviour than the trailing cavity. The spectral characteristics of the turbulence intensity of the trailing cavity shear layers are similar to those of the leading cavity shear layers. The corresponding results are therefore not presented.

As the offset distance is reduced, the difference between the mean flow speed and turbulence intensity profiles is also reduced (not shown here). However, the corresponding results are largely inline with those shown in Figs. 2 to 4 and thus they are not discussed further.

B. Sound transmission loss

The sound transmission loss, *TL*, is defined as

$$TL = 20\log_{10}\left|\frac{T}{I}\right|, \tag{1}$$

where I and T are the amplitude of the incident wave (upstream of the coupled cavities) and the transmitted wave respectively. Figure 5 shows the spectral variations of the *TL*s across the coupled cavity regions with different offset ratios δ_r (= δ/w) and cavity lengths. The two coupled cavities form a regular expansion chamber when δ_r = 0, and they are 100% offset when δ_r = 1. The finite-element simulation results[18,20] of the corresponding 100% offset cases are included for comparison.

It should be noted that the TLs for frequency higher than $0.86f_1$ fluctuate significantly because of the cut-on of the first spanwise higher mode ($w/s = 0.86$), while the multiple microphone method adopted in this study caters only for planar modes. Though the test section was made essentially two-dimensional, a very small misalignment in the spanwise direction could result in such phenomenon. This is also the situation when a duct flow is introduced because of the three-dimensional flow turbulence even if the test section is made perfectly two-dimensional. Results at frequency above $0.85f_1$ are thus ignored in the present study. It is also not the purpose of this study to examine the condition at higher frequencies as the stopbands of the coupled cavities are well below the first transverse higher mode frequency of the duct.[20] Shallow cavities, like those addressed by Oshkai et al.,[32] are not within the scope of this study.

In general, the TL magnitude increases with increasing offset distance and there is a slight increase in the frequency of peak sound transmission loss, f_p, at the same time. The strong peak is found to be the result of the strong pressure-releasing effect of the first transverse acoustic mode in the middle region of the cavity section.[20] One can notice that the magnitude of the peak TL reduces with decreasing cavity length for all offset ratios. This is not surprising as the TL of a regular expansion chamber decreases with chamber length for a fixed area expansion ratio when the chamber length is less than a quarter of the excitation wavelength.[9]

There are some discrepancies between the $\delta/w = 1$ results obtained by finite-element method and experiment. However, the difference in the TL peak frequency is just about 3 – 4 %, and similar discrepancy is not really significant (for instance, Wang et al.[33] and Zhao et al.[34]). The spectral variation trends of the results obtained by the two approaches are very similar. It will be shown later that the present obtained sound pressure fluctuation patterns within the two cavities also agree with those predicted by Tang and Tang.[20]

Figure 6 illustrates the spectral variation of phase differences between microphones M5 and M6 for $w/a = 2/3$. These microphones capture the sound pressure fluctuations deep inside the cavities. It can be observed that a substantial phase change around ~$0.63f_1$ is already excited even at $\delta_r = 0$.

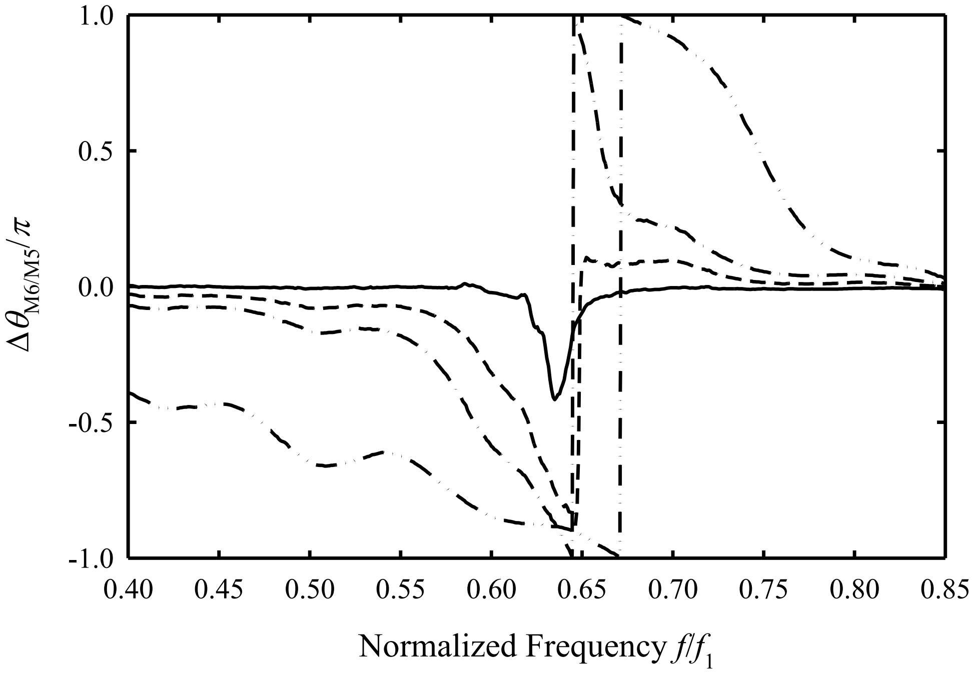

FIG. 6. Phase difference between signals at M5 and M6. U = 0 m/s, w/a = 2/3.
———— : δ_r = 0; – – – – : δ_r = 0.1; —·— : δ_r = 0.2; —··— : δ_r = 1.

The increase in δ_r results in strong out-of-phase pressure fluctuations within the two cavities near to f_p, which again agrees with the numerical simulation of Tang and Tang.[20] Similar phenomena are observed for w/a = 7/15 and thus the corresponding results are not presented.

One should note that the actual sound pressure spectra inside the duct and the cavities are not useful as their shapes are dictated by the spectrum of the excitation sound radiated out from the loudspeaker. Therefore, frequency response functions are used hereinafter to relate the sound pressures within the cavities to the incident sound wave from upstream of the cavities. Following the two-microphone method of Chung and Blaser,[28] one can establish, for plane wave motions, before swapping the two wall-mounted microphones M1 and M2, in the frequency domain,

$$p_1 = Ie^{-j\frac{k}{1+M}} + Re^{j\frac{k}{1-M}x_1},\ p_2 = \left(Ie^{-j\frac{k}{1+M}x_2} + Re^{j\frac{k}{1-M}x_2}\right)e^{j\phi_2},\ p_s = Se^{j\phi_s}, \qquad (2)$$

where $j = \sqrt{-1}$, M the Mach number of the duct flow, p_1, p_2 and p_s denote the signals recorded by M1, M2 and a sensor within the coupled cavity S respectively, k the wavenumber, x_1 and x_2 the axial locations of M1 and M2 respectively, I, R and S the magnitudes of the upstream incident wave, upstream reflected wave and the signal measured by sensor S respectively. The angles ϕ_2 and ϕ_S represent the phase responses of M2 and S with reference to signals at M1 respectively. The amplitude responses of the measurement devices are different, but they have been taken into account by calibration already. After swapping M1 and M2, one obtains

$$p_1 = \left(Ie^{-j\frac{k}{1+M}x_2} + Re^{j\frac{k}{1-M}x_2}\right)e^{j\alpha},\ p_2 = \left(Ie^{-j\frac{k}{1+M}x_1} + Re^{j\frac{k}{1-M}x_1}\right)e^{j(\phi_2+\alpha)},\ p_s = Se^{j(\phi_s+\alpha)}, \quad (3)$$

where α is a general phase variation between the above two sets of measurements (Eqs. 2 and 3). The target here is to estimate the transfer function / frequency response, $H_{I,S} = S/I$. One can find from Eqs. (2) and (3) that

$$H_{I,S} = \frac{S}{I} = H_{1,S}e^{-j\left(\phi_s + \frac{k}{1+M}x_1\right)}\left(1 - \frac{\sqrt{H'_{2,1}H_{1,2}} - e^{-j\frac{k}{1+M}\Delta}}{\sqrt{H'_{2,1}H_{1,2}} - e^{j\frac{k}{1-M}\Delta}}\right), \quad (4)$$

where $\Delta = |x_1 - x_2|$, $H_{i,j}$ denotes the transfer function p_j/p_i and $'$ represents the quantity associated with the swapped microphone measurement. The argument kx_1 of the exponential function is arbitrary and ϕ_s is unknown. However, one can ignore x_1 as the present analysis is done with reference to the signal at M1. Eq. (4) is useful as the magnitude of $H_{S,I}$ is a main concern in the present study. It should be noted that the incident sound pressure magnitude I, which represents also the artificial excitation level, can be estimated using $H_{M1,I}$ together with the sound pressure recorded at M1. In the foregoing discussions, I is given in decibels.

Two examples of the frequency response functions $H_{M5,I}$ and $H_{M6,I}$ for $w/a = 2/3$, $I \sim 87.8$ dB are presented in Fig. 7(a). It is noticed that resonance occurs inside both cavities and the magnitude of the corresponding sound pressure inside the leading cavity is higher than that inside the trailing cavity regardless of the offset ratio. Both sound pressures are stronger than the incident wave. It can also be observed that the resonance frequency of the leading cavity is higher than that of the trailing cavity and both of these frequencies are lower than the corresponding peak *TL* frequencies f_p. For the leading cavity, the sound pressure (M5) is actually in-phase with the incident sound at resonance, while for the trailing cavity, phase lag of $\pi/2$ and $3\pi/4$ are recorded for $\delta_r = 1$ and 0.5 respectively. It is obvious that such phase differences of the cavity pressures cannot result in complete cancellation of the incident wave. The highest *TL* is achieved when the cavity pressures are out-of-phase with

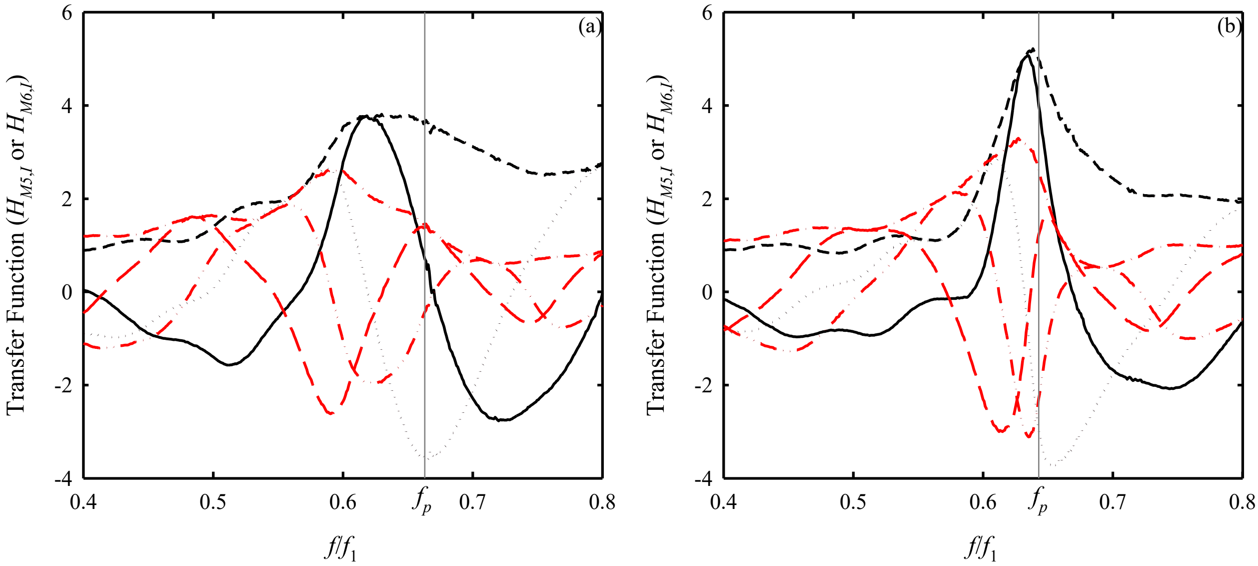

FIG. 7. (Color online) The complex sound pressures within cavities. $U = 0$ m/s.
(a) $w/a = 2/3$, $\delta_r = 1$, $I = 87.8$ dB; (b) $w/a = 7/15$, $\delta_r = 1$, $I = 101.0$ dB.
——— : Real($H_{M5,I}$); ········· : Imag($H_{M5,I}$); – – – – : | $H_{M5,I}$ |;
— ·· — : Real($H_{M6,I}$); — — : Imag($H_{M6,I}$); — · — : | $H_{M6,I}$ |.

each other, while none of them is in-phase with the incident wave. This condition is achieved at a frequency higher than the cavity resonance frequencies.

Besides, cavity resonance is stronger at lower δ_r (except when $\delta_r \equiv 0$) because of the stronger resonance of the odd transverse dual cavity chamber mode as shown in Tang and Tang.[20] However, stronger cavity pressures are associated with a lower *TL*. Too strong cavity pressures could result in extra sound power radiation downstream, reducing the overall *TL*. The results with $w/a = 7/15$, which are shown in Fig. 7(b), are very much inline with those of $w/a = 2/3$. Therefore, they are not discussed. The strength of the artificial excitation does not affect the results in the absence of a duct flow.

The presence of a low Mach number flow along the duct results in flow separations at the sharp edges of the cavities, and these shear flows could cause pressure fluctuations in the coupled cavity region, affecting the overall acoustical impedance and thus the sound propagation and sound transmission loss. These shear flows could also be sound producing (for instance, Davies and Holland,[22] Rossiter[35] and Tonon et al.[23,36]). It should be noted that the flow Mach number in the present study is well below 0.1. The effect of mean flow Mach number in the calculation of all the required transfer functions (Eq. 4) and *TL* is negligible.

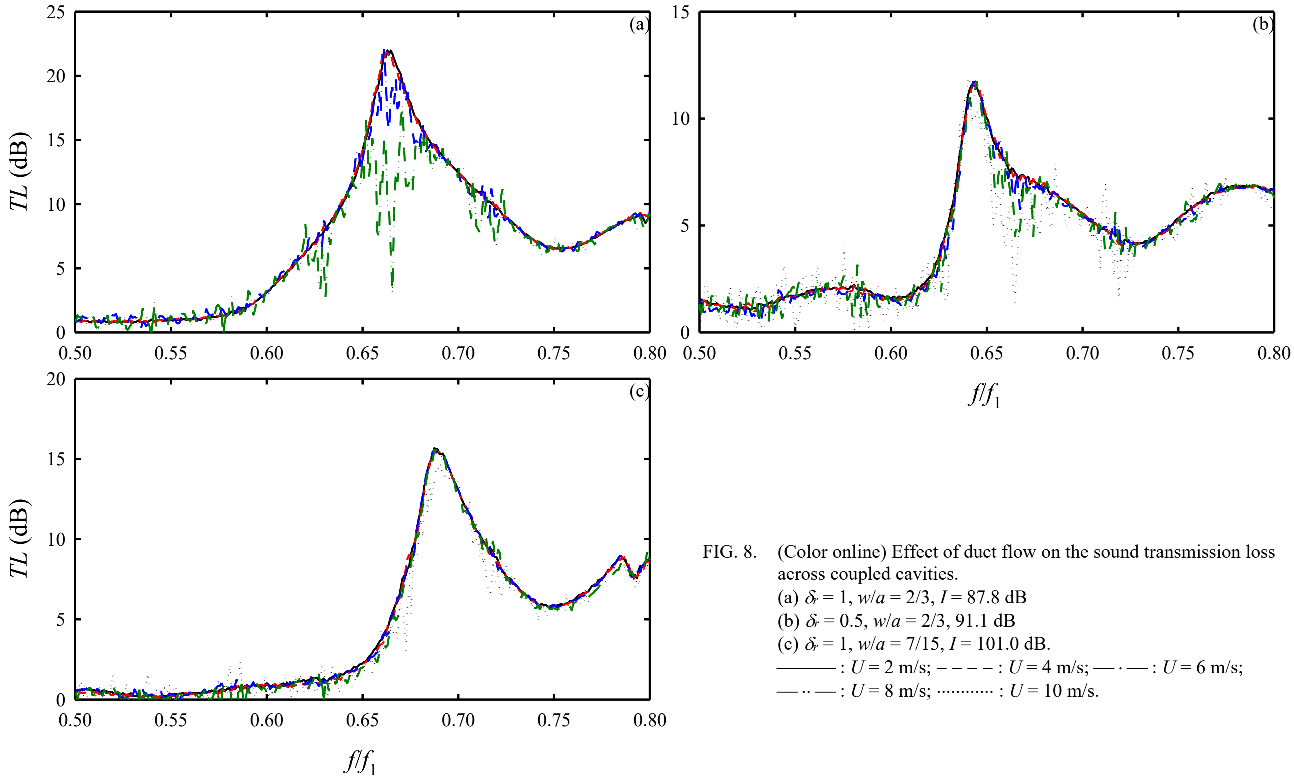

FIG. 8. (Color online) Effect of duct flow on the sound transmission loss across coupled cavities.
(a) $\delta_r = 1$, $w/a = 2/3$, $I = 87.8$ dB
(b) $\delta_r = 0.5$, $w/a = 2/3$, 91.1 dB
(c) $\delta_r = 1$, $w/a = 7/15$, $I = 101.0$ dB.
——— : $U = 2$ m/s; – – – – : $U = 4$ m/s; — · — : $U = 6$ m/s; — ·· — : $U = 8$ m/s; ············ : $U = 10$ m/s.

Figure 8 illustrates some examples of the *TL* reductions upon the introduction of a low Mach number flow into the present duct. For $w/a = 2/3$ and $\delta_r = 1$, significant *TL* reduction is observed after the mean flow speed *U* exceeds 4 m/s [Fig. 8(a)], while such phenomenon is observed at a higher *U* at $\delta_r = 0.5$ with the same w/a [Fig. 8(b)]. As the sound pressures inside the cavities are stronger at decreased δ_r (Fig. 7), it is believed that the *TL* drop will decrease with stronger sound pressures and thus decreasing δ_r at a fixed *U*. This will be discussed further later.

Figure 8(c) shows the *TL* reductions for the case of $w/a = 7/15$, $\delta_r = 1$ and $I = 101.0$ dB. Again, significant *TL* drop appears at $U > 8$ m/s. It should be noted that the sound pressures inside the cavities with $w/a = 7/15$ are also higher than those in the case of $w/a = 2/3$. This adds further to the possibility of a lower *TL* drop is associated with a stronger cavity sound pressures.

The magnitudes of $H_{M5,I}$ and $H_{M6,I}$ at $w/a = 2/3$, $\delta_r = 1$ and $I = 87.8$ dB with $U = 2$ m/s and 8 m/s are presented in Fig. 9(a). The results of the 'no flow' case basically collapse with those with $U = 2$ m/s and thus are not presented. The introduction of the duct flow tends to increase the strength of the cavity sound pressures at $U = 8$ m/s. The effect is mainly concentrated at and around the *TL* peak frequencies because the cavity shear layers are strongly excited within this frequency band.

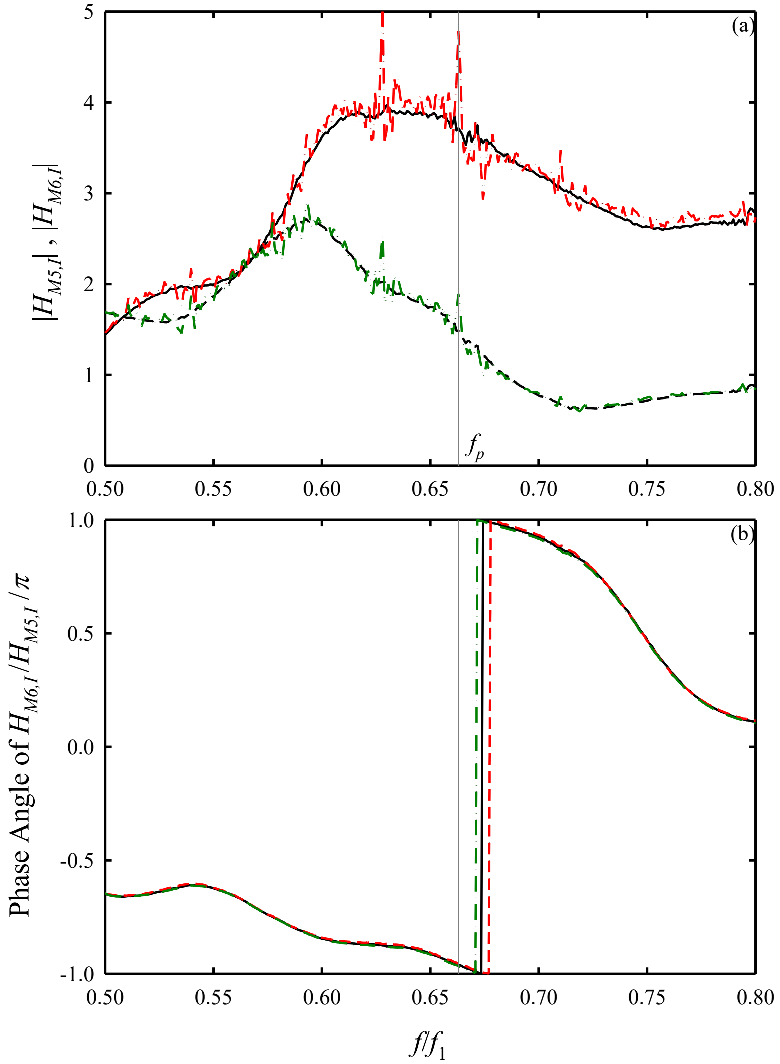

FIG. 9. (Color online) Cavity pressure transfer functions in the presence of a duct flow. $\delta_r = 1$; $w/a = 2/3$; $I = 87.8$ dB.
(a) Magnitudes of transfer functions;
——— : $|H_{M5,1}|$, $U = 2$ m/s; – – – – : $|H_{M6,1}|$, $U = 2$ m/s;
— · — : $|H_{M5,1}|$, $U = 8$ m/s; — ·· — : $|H_{M6,1}|$, $U = 8$ m/s.
(b) Phase differences between transfer functions;
– – – – : $U = 0$ m/s; ——— : $U = 2$ m/s; — · — : $U = 8$ m/s.

Sharp peaks near to f_p can be found in both transfer functions. It appears that a sharp pressure peak at M5 is associated with a *TL* dip. It will be shown later that this peak is due to the aeroacoustical interference within the cavity region. The peak at ~$0.62f_1$ is also believed to be due to such interference. However, the corresponding *TL* is low and thus it is not considered further in this study. It should be noted that the strong sound pressures inside the cavities compared to the incident sound level could lead to the nonlinear roll-up of tiny discrete vortices at the interfaces between the cavities and the main duct flow.[37] Linear instability theory[38] could fail in the present circumstance.

It is observed from Fig. 9(a) that the increase in the sound pressure in the leading cavity is higher than that in the trailing cavity at these pressure peaks. The phase difference between M5 and

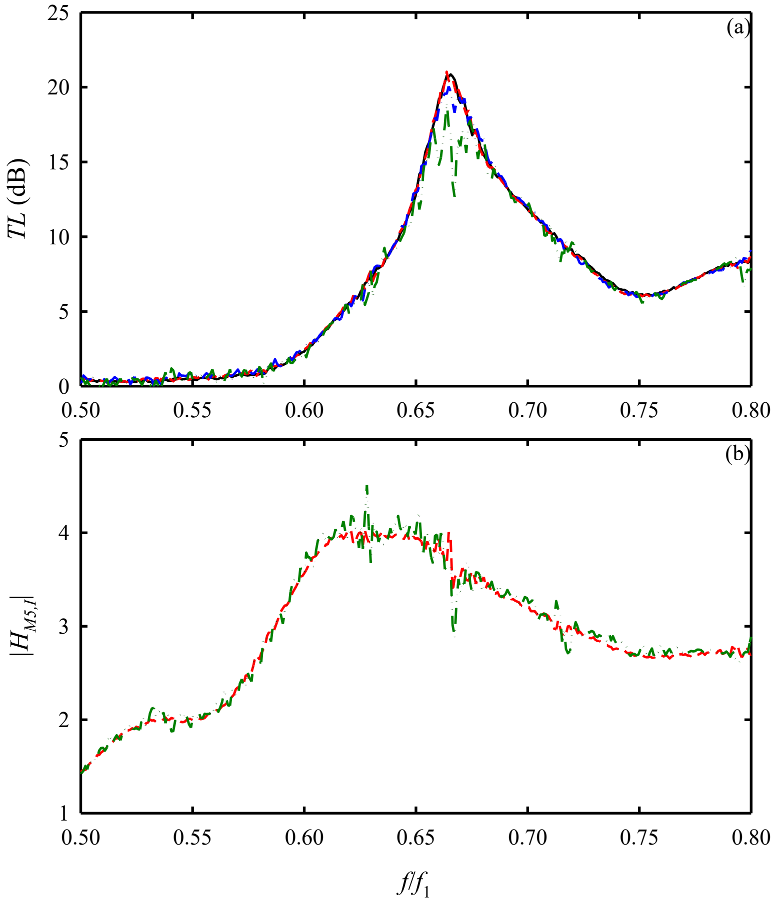

FIG. 10. (Color online) Cavity pressure transfer functions in the presence of a duct flow at stronger excitation.
$\delta_r = 1$; $w/a = 2/3$; $I = 99.2$ dB.
(a) *TL*; (b) $|H_{M5,I}|$.
———— : $U = 0$ m/s; – – – – : $U = 6$ m/s; — · — : $U = 8$ m/s; — ·· — : $U = 10$ m/s.

M6 at f_p is not changed much when U is increased from 0 m/s to 8 m/s [Fig. 9(b)] though the frequency of out-of-phase cavity pressure is shifted slightly higher with the increase of U. The stronger increase in the leading cavity pressure disturbs the pressure balance originally found in the 'no flow' case, resulting in less efficient cancelling wave or even extra sound radiation out of the coupled cavity region and reducing the *TL*. Similar phenomenon, though is less remarkable, can be found in other coupled cavities tested in the present study and thus the corresponding results are not presented.

One can infer from the results discussed in Sec. III.A that the strength of the incident sound I relative to those of the shear layers will have an effect on the *TL* in the presence of a low Mach number duct flow. Figure 10 illustrates the spectral variations of the *TL* across the coupled cavities with $w/a = 2/3$, $\delta_r = 1$ at different mean flow speeds under an excitation 10 dB in general higher than that adopted in Figs. 8(a) and 8(b). It is observed that significant *TL* drop is found only when U is increased beyond 6 m/s in the presence of a stronger incident sound. The *TL* drop at U = 10 m/s in this case is even smaller than that at U = 8 m/s under the weaker excitation case [Fig. 8(a)]. A higher U results in a stronger shear rate across the shear layers, increasing the strength of the shear layer. It is evidenced that under a stronger incident sound excitation, a higher U is required to produce shear layers aeroacoustically powerful enough to affect the sound field in the coupled cavity region.

The corresponding $|H_{M5,I}|$s are presented in Fig. 10(b). For the sake of clarity, only those at U = 6 m/s and 10 m/s are given. The $|H_{M5,I}|$ at U = 6 m/s is nearly the same as that of the 'no flow' case and that presented in Fig. 9(a) at U = 2 m/s obtained under a lower incident sound level. However, the kind of strong sharp spikes (dips) observed in Fig. 9(a) at U = 6 m/s are found at U = 10 m/s for the case of a stronger upstream excitation [Fig. 10(b)]. Similar observations apply to the case of $|H_{M6,I}|$ and thus the corresponding data are not presented. These results are consistent with the above deduction that the sound fields inside the cavities under a stronger upstream acoustic excitation can only be affected by stronger shear layers (thus, a higher U). One should also note that the responses of the leading cavity are nearly independent of the flow velocity U.

Since the *TL* dips in the presence of the low Mach number flows are relatively broadband compared to the *TL* peaks due to the offset cavities, the *TL* reduction in the presence of the flows, ΔTL, will be described using the 1/24th band *TL*s with f_ps as the band centre frequencies in the foregoing analysis. Under the present f_ps, the bandwidth of this averaging is about 25 Hz. Some examples showing the dependence of ΔTL with incident sound pressure amplitude and offset ratio are presented in Fig. 11. One can observe that the ΔTLs for $U \leq 4$ m/s are basically negligible. However, there exists a critical U over which the *TL* reduction (that is, ΔTL) increases quickly with increasing U and such increase is quite linear for $U < 16$ m/s. The rate of such increase is faster at lower incident sound level for a fixed configuration of the coupled cavities. It also increases with increasing offset ratio under a fixed upstream excitation level and w. For a shorter cavity, the rate of ΔTL increase with U increases faster with reducing offset ratio than in the case of the longer cavity. It is noticed that the increase of ΔTL with U could slow down when U exceeds 16 m/s. However, the

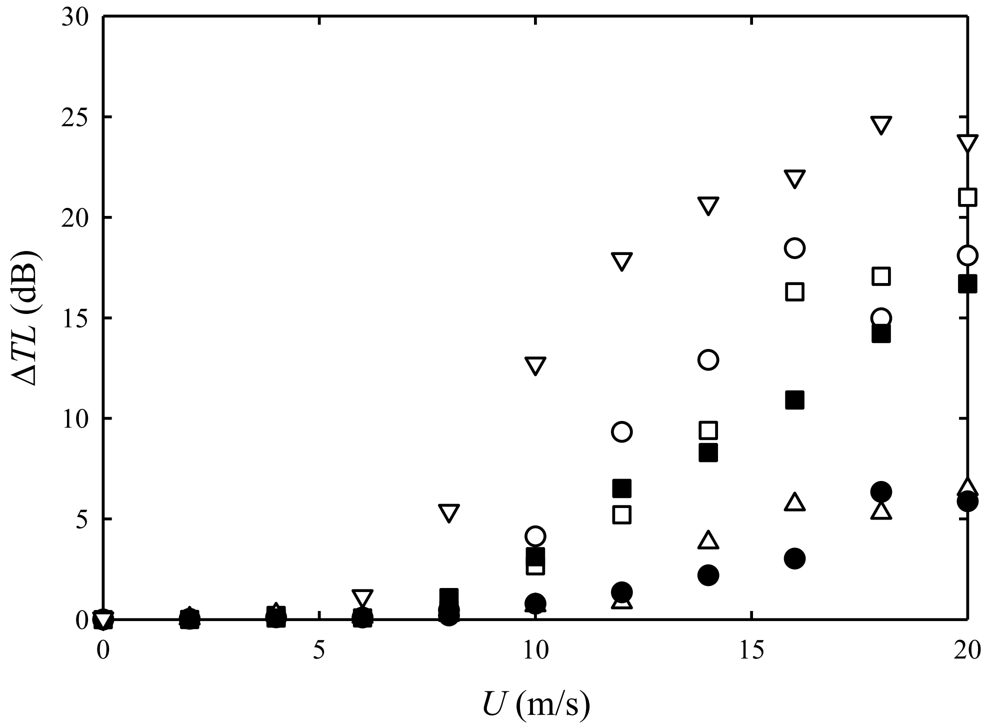

FIG. 11. Some examples of the variation of ΔTL with U.
○ : $L/w = 2/3$, $\delta_r = 0.6$, $I = 91.8$ dB; △ : $L/w = 2/3$, $\delta_r = 0.6$, $I = 101.0$ dB;
▽ : $L/w = 2/3$, $\delta_r = 0.6$, $I = 82.4$ dB; □ : $L/w = 2/3$, $\delta_r = 1$, $I = 99.2$ dB
● : $L/w = 7/15$, $\delta_r = 6/7$, $I = 101.0$ dB; ■ : $L/w = 7/15$, $\delta_r = 4/7$, $I = 85.8$ dB

results in this range of flow speed is not going to be useful because of the plausible contamination due to flow turbulence. In the foregoing analysis, an attempt is made to relate the abovementioned critical flow speed, U_{cr}, and f_p, which depends the configuration of the coupled cavities. As shown in Fig. 8, this U_{cr} increases upon stronger artificial excitation. It also increases with decreasing offset ratio and increasing cavity length.

C. Critical flow speeds, Strouhal numbers and the related length scale

Figure 12 illustrates schematically how the U_{cr}s are determined in the present study. The region of linear (approximately) increase of ΔTL with U is first identified. The best straight line is then established using the least square method and the interception of this line on the $\Delta TL = 0$ dB axis gives U_{cr}. One should note that there could be error in the estimation of U_{cr} as the choice of the abovementioned linear region could be a bit arbitrary, especially for cases where the artificial excitation levels are around the lower bound in this study. However, repeated trials suggest that the error is at maximum ~5%.

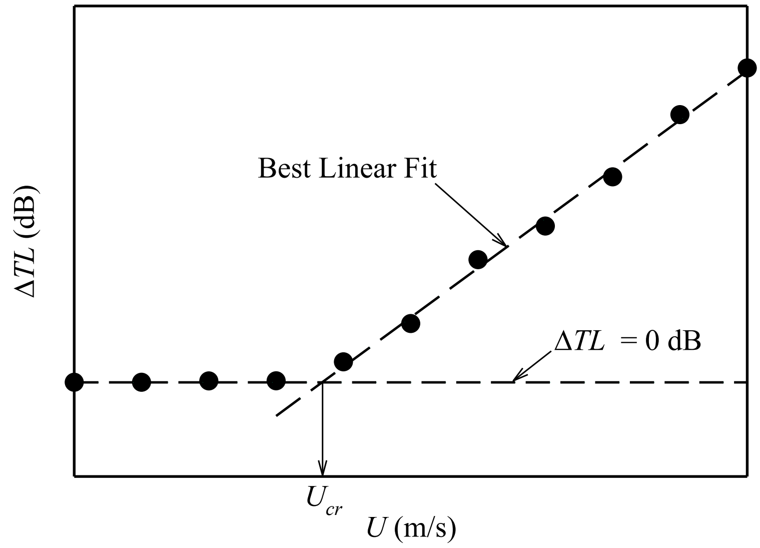

FIG. 12. Schematic for the determination of U_{cr}.
■ : w/a = 7/15, δ_r = 4/7, I = 85.8 dB.

The variations of $U_{cr}/(wf_p)$ with δ_r are presented in Fig. 13. The corresponding results at δ_r less than 0.1 are not presented as the TL peaks in those cases cannot be identified reliably, though one can still approximate the corresponding f_ps using the formula of Tang and Tang[20] or the phase difference between signals at M5 and M6 (c.f. Fig. 6). One can notice that $U_{cr}/(wf_p)$ tends to decrease fairly linearly with increasing offset ratio regardless of the artificial excitation level and the cavity length. The best straight lines obtained again using the method of least square are also given in Fig. 13. More interesting is that the results of the linear fit suggest that a new kind of similitude exists in the aeroacoustics of coupled cavities with a definite relationship between $U_{cr}/(wf_p)$ and δ_r :

$$\frac{U_{cr}}{wf_p} \approx \alpha(\beta - \delta_r), \tag{6}$$

where the slope α depends on excitation level and cavity length, while β just varies within a narrow range from 1.83 to 2.17, which is ~ 2 on average. One can also notice that α decreases with decreasing artificial excitation level and a shorter cavity results in smaller α.

One can then derive a critical Strouhal number, St_{cr}, based on a new length scale L_e equals (β − δ_r)w, such that

$$St_{cr} = \frac{f_p L_e}{U_{cr}} = \frac{f_p}{U_{cr}}(\beta - \delta_r)w = \frac{f_p}{U_{cr}}(\beta w - \delta) = \frac{1}{\alpha}. \tag{7}$$

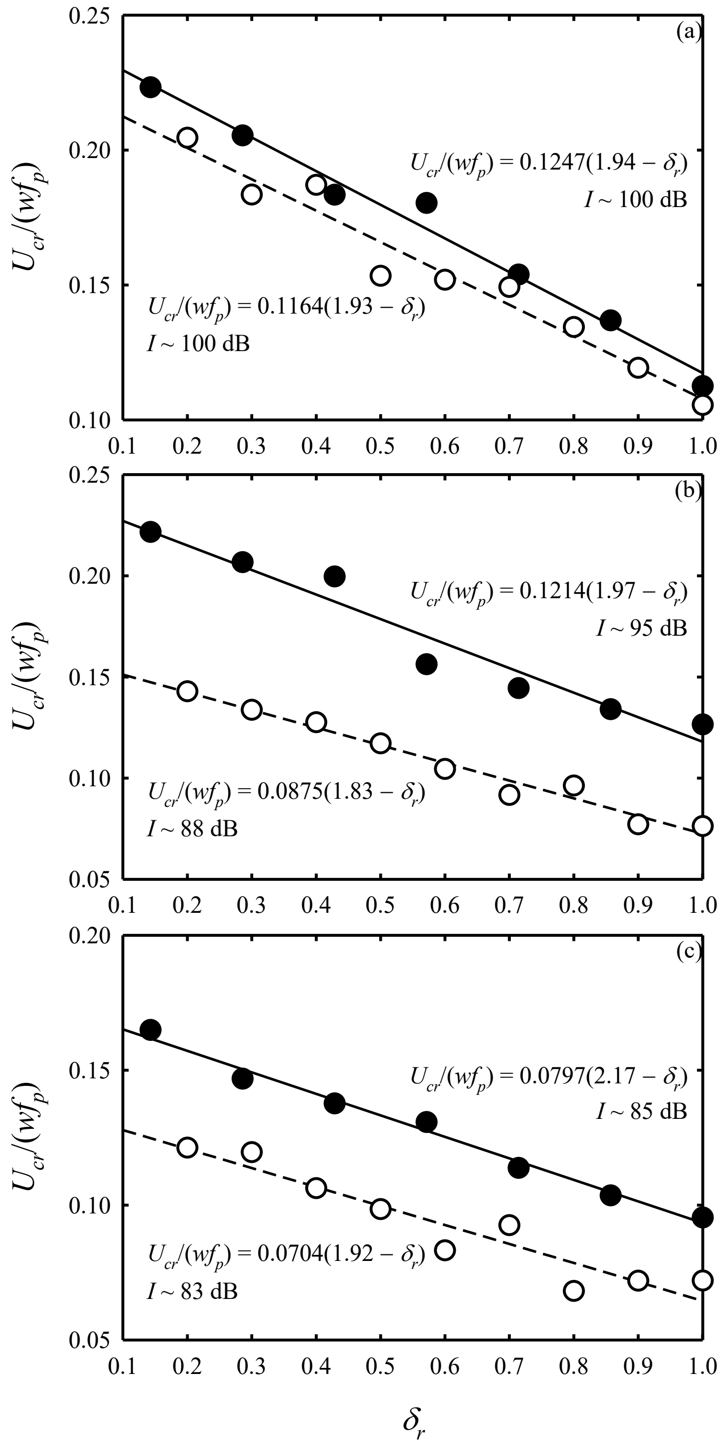

FIG. 13. Variations of $U_{cr}/(wf_p)$ with δ_r under different excitation levels.
(a) Strong excitation; (b) medium excitation; (c) weak excitation.
○ : w/a = 2/3; ● : w/a = 7/15;
——— : regression line for w/a = 7/15; – – – – : regression line for w/a = 2/3.

St_{cr} thus increases with decreasing cavity length or artificial excitation level. A summary of the relationship between St_{cr}, I, w/a and β are given in Table I. As f_p does vary within a narrow range for a fixed w/a while δ_r should also have some effects on the acoustical impedance of the coupled cavities, the excitation level I does vary over a small range in the present study even for a fixed

TABLE I. Summary of $U_{cr}/(wf_p)$ against δ_r.

w/a	I (dB)	β	α	St_{cr} (=1/α)	γ (= 1/β)
7/15	99.7 ± 1.3	1.9413	0.1247	8.02	0.52
	96.4 ± 2.0	1.9708	0.1214	8.23	0.51
	85.2 ± 1.0	2.1710	0.0797	12.54	0.46
2/3	100.1 ± 0.9	1.9263	0.1164	8.59	0.52
	90.5 ± 1.3	2.0245	0.0886	11.29	0.49
	87.8 ± 0.8	1.8287	0.0875	11.43	0.55
	82.5 ± 1.3	1.9162	0.0704	14.21	0.52

electrical power fed to the loudspeaker. It is noticed that St_{cr} tends to decrease with I. It is rather expected as a stronger shear rate is required to create a pressure fluctuation which is capable of affecting that due to an elevated artificial excitation level. As f_p does not change much in the presence of a duct flow for a fixed coupled cavity system, the increase in shear rate, which is achieved through an increase in the flow speed U, results in a lower Strouhal number. St_{cr} is around 8 at high excitation of ~100 dB regardless of w/a. Figure 14 indicates that there is very likely a definite simple relationship between St_{cr} and I which could be independent of w/a. The strength and the aerodynamics of the shear layers and the artificial excitation level should play crucial roles in the underlying mechanism. Further investigations are needed for deeper understanding of this

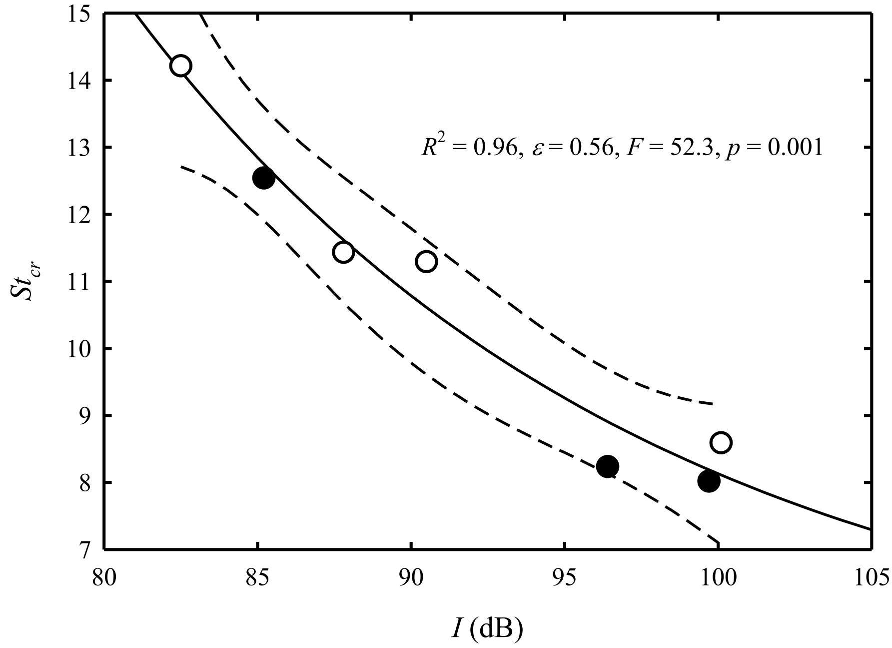

FIG. 14. Variation of St_{cr} with excitation level.
○ : L/w = 2/3; ● : L/w = 7/15;
——— : regression line (exponential form);
– – – – : 95% confidence bounds.

aeroacoustic behaviour and the actual relationship between St_{cr} and I. Since f_p can be estimated using the method given in Tang and Tang,[20] this new St_{cr} formulation (Eq. 7) can in principle be used to determine, for a fixed coupled cavity configuration and excitation level, the flow speed over which significant TL drop is expected. The physics which leads to such a length scale L_e is left to further investigations.

IV. CONCLUSIONS

A series of experiments was conducted in the present study in an attempt to understand the mechanism leading to the strong sound transmission loss across two coupled cavities along a rectangular duct. The present coupled cavity system was formed by offsetting the two cavities that made up a conventional expansion chamber. The effects of a low Mach number duct flow on the reduction of the sound transmission loss were also studied in details. For practical application reasons, the dimensions of the cavities adopted were small compared to those of the main duct.

In the absence of the duct flow, broadband increase in the sound transmission loss is observed when the two cavities of a conventional expansion chamber are offset. A peak on the sound transmission loss spectrum is also observed at the same time, and the frequency of this peak is higher than the resonance frequency of each cavity. The magnitude of this peak sound transmission loss increases with increasing degree of cavity offset, but its frequency does not vary much though it does show an increasing trend with increasing offset distance. The performance of the coupled cavities is independent of the artificial excitation level.

The sound transmission loss across the coupled cavities is lowered upon the introduction of the low Mach number duct flow. For any degree of cavity offset, there is a flow speed below which the sound transmission loss remains fairly unchanged. A new length scale is established. This new length scale, together with the critical flow speed and the peak sound transmission loss frequency, gives a Strouhal number, which is independent of the offset ratio, for a fixed cavity length. This dimensionless Strouhal number decreases with increasing excitation level, but does not depend much on the cavity length. All of these collectively suggest that similitude exists in the present low Mach number aeroacoustic problem. The working frequency range and the flow speed limit of coupled cavities as duct silencer are therefore predictable based on such similitude.

ACKNOWLEDGEMENT

This work is supported by a grant from the Research Grant Council, the Hong Kong Special Administration Region Government under Project number PolyU5271/11E.

[1] K.D. Kryter, *The Effects of Noise on Man* (Academic, New York, 1985).

[2] L.L. Beranek, "Criteria for office quieting based on questionnaire rating studies," J. Acoust. Soc. Am. **28**, 833 – 852 (1956).

[3] B. Hay and M.F. Kemp, "Measurement of noise in air conditioned landscape offices," J. Sound Vib. **23**, 363 – 373 (1972).

[4] C.M. Harris, *Handbook of Noise Control* (McGraw-Hill, New York, 1979).

[5] L. Huang and Y.S. Choy, "Vibroacoustics of three dimensional drum silencer," J. Acoust. Soc. Am. **118**, 2313 – 2320 (2005).

[6] S. Allam and M. Åbom, "A new type of muffler based on microperforated tubes," ASME Trans. J. Vib. Acoust. **133**, 031005 (2011).

[7] G. Canevet, "Active sound absorption in an air conditioning duct," J. Sound Vib. **58**, 333 – 345 (1978).

[8] U. Ingard, "On the theory and design of acoustic resonators," J. Acoust. Soc. Am. **25**, 1037 – 1061 (1953).

[9] M.L. Munjal, *Acoustics of Ducts and Mufflers* (Wiley, New York, 1987).

[10] A. Salemat, N.S. Dickey and J.M. Novak, "The Herschel-Quincke tube : A theoretical, computational and experimental investigation," J. Acoust. Soc. Am. **96**, 3177 – 3185 (1994).

[11] T. Kar and M.L. Munjal, "Analysis and design of conical concentric tube resonators," J. Acoust. Soc. Am. **116**, 74 – 83 (2004).

[12] S.H. Seo and Y.H. Kim, "Silencer design by using array resonators for low frequency band noise reduction," J. Acoust. Soc. Am. **118**, 2332 – 2338 (2005).

[13] C.Q. Howard, B.S. Cazzolato and C.H. Hansen, "Exhaust stack silencer design using finite element analysis," Noise Control Eng. J. **48**, 113 – 120 (2000).

[14] C.Q. Howard and R.A. Craig, "Noise reduction using a quarter wave tube with different orifice geometries," Appl. Acoust. **76**, 180 – 186 (2014).

[15] S.K. Tang, "Narrow sidebranch arrays for low frequency duct noise control," J. Acoust. Soc. Am. **132**, 3086 – 3097 (2012).

[16] H.M.Yu and S.K. Tang, "Sound transmission loss across a narrow sidebranch array duct muffler at low Mach number," J. Acoust. Soc. Am. **148**, 1692 – 1702 (2020).

[17] M. Červenka and M. Bednařík, "Optimized reactive silencers with narrow side-branch tubes," J. Acoust. Soc. Am. **144**, 2015 – 2021 (2018).

[18] S.K. Tang and Y.J. Tang, "Sound transmission across expansion chambers with staggered sub-chambers in a low Mach number duct," Proc. INTERNOISE 2015 San Francisco, USA (2015).

[19] R.C.K. Leung, R.M.C. So, S.K. Tang and X.Q. Wang, "Passive duct noise control by enhancing aeroacoustic interference due to side-branch discontinuities," J. Sound Vib. **330**, 3316 – 3333 (2011).

[20] Yijia Tang and S.K. Tang, "On low frequency sound propagation across closely coupled narrow cavities along an infinite duct and the similarity in stopband cut-on frequency," J. Sound Vib. **443**, 411 – 429 (2019).

[21] S.K. Tang, "On sound transmission loss across a Helmholtz resonator in a low Mach number flow duct," J. Acoust. Soc. Am. **127**, 3519 – 3525 (2010).

[22] P.O.A.L. Davies and K.R. Holland, "The observed aeroacoustic behaviour of some flow-excited expansion chambers," J. Sound Vib. **239**, 695 – 708 (2001).

[23] D. Tonon, B.J.T. Landry, S.P.C. Belfroid, J.F.H. Willems, G.C.J. Hofmans and A. Hirschberg, "Whistling of a pipe system with multiple side branches : Comparison with corrugated pipes," J. Sound Vib. **329**, 1007 – 1024 (2010).

[24] L.L. Beranek, *Noise and Vibration Control Engineering, Principles and Applications* (Wiley, New York, 1992), Chap. 10.

[25] P.A. Nelson, N.A. Halliwell and P.E. Doak, "Fluid dynamics of a flow excited resonance, Part I : Experiment," J. Sound Vib. **78**, 15 – 38 (1981).

[26] W. Neise, W. Frommhold, F.P. Mechel and F. Holste, "Sound power determination in rectangular flow ducts," J. Sound Vib. **174**, 201 – 237 (1994).

[27] S.K. Tang and F.Y.C. Li, "On low frequency sound transmission loss of double sidebranches: A comparison between theory and experiment," J. Acoust. Soc. Am. **113**, 3215 – 3225 (2003).

[28] J.Y. Chung and D.A. Blaser, "Transfer function method of measuring acoustic intensity in a duct system with flow," J. Acoust. Soc. Am. **68**, 1570 – 1577 (1980).

[29] S.K. Tang and N.W.M. Ko, "Coherent structure interactions in an unexcited coaxial jet," Expts. Fluids **17**, 147 – 157 (1994).

[30] I. Wygnanski and H.E. Fiedler, "The two-dimensional mixing region," J. Fluid Mech. **41**, 327 – 361 (1970).

[31] B.G. Jones, R.J. Adrian and C.K. Nithianandan, "Spectra of turbulent static pressure fluctuations in jet mixing layers," AIAA J. **17**, 449 – 457 (1979).

[32] P. Oshkai, D. Rockwell and M. Pollack, "Shallow cavity flow tones: transformation from large- to small-scale modes," J. Sound Vib. **280**, 777 – 813 (2005).

[33] J. Wang, P. Rubini and Q. Qin, "A porous media model for the numerical simulation of acoustic attenuation by perforated liners in the presence of grazing flows," Appl. Sci. **11**, 4677 (2021).

[34] H. Zhao, Z. Lu, Y. Guan, Z. Liu, G. Li, J. Liu and C.Z. Ji, "Effect of extended necks on transmission loss performances of Helmholtz resonators in the presence of a grazing flow," Aerosp. Sci. Technol. **77**, 228 – 234 (2018).

[35] J.E. Rossiter, Wind-tunnel experiments on the flow over rectangular cavities at subsonic and transonic speeds, Aero. Res. Counc. R. & M. no. 3438 (1964).

[36] D. Tonon, A. Hirschberg, J. Golliard and S. Ziada, "Aeroacoustics of pipe systems with closed branches," Int. J. Aeroacoust. **10**, 201 – 276 (2011).

[37] G. Kooijman, A. Hirschberg and J. Golliard, "Acoustical responses of orifices under grazing flow : Effect of boundary layer profile and edge geometry," J. Sound Vib. **315**, 849 – 874 (2008).

[38] A. Michalke, "On spatially growing disturbances in an inviscid shear layer," J. Fluid Mech. **23**, 521 – 544 (1965).